

Almost Perfect Reconstruction Filter Bank for Non-redundant, Approximately Shift-Invariant, Complex Wavelet Transforms

Reshad Hosseini

*Biomedical Engineering, Amirkabir University of Technology
Tehran, Iran 15875–4413
E-mail: r.hosseini@aut.ac.ir*

Mansur Vafadust

*Faculty of Biomedical Engineering, Amirkabir University of Technology
Tehran, Iran 15875–4413
E-mail: vmansur@aut.ac.ir*

Abstract

This paper presents a new filter bank design technique which leads to the shift-invariant representation of signals. The proposed wavelet transform due to the specific power spectrum of its filters has oriented filters in higher dimensions. Unlike previous approaches, its filters do not have serious distributed bumps in the wrong side of the power spectrum and, simultaneously, they do not introduce any redundancy to the original signal. The proposed filter bank has linear phase filters and high vanishing moment property. The simulation results show promising properties of the proposed filter bank that can be exploited in different signal processing applications.

AMS Subject Classification:

Keywords:

1. Introduction

It is well known that the traditional, separable discrete wavelet transform (DWT) is optimum for point singularities and therefore optimum for 1-D signals. But this transform is not optimum in higher dimensions. For example in the case of 2-D transform, the filters are not oriented and they mix $+45^\circ$ and -45° angles. Another deficiency of DWT is that its coefficients are variant with a little shift in the input signal.

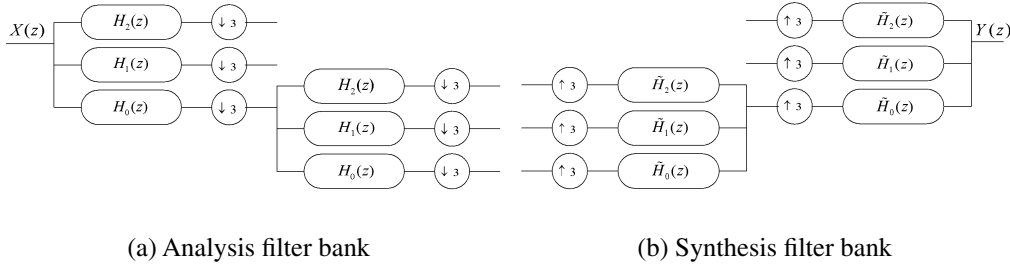


Figure 1: The 3-Band analysis and synthesis filter banks for the orthogonal wavelet.

There are some papers in the literature addressing these deficiencies of the common wavelet transform [1]. It was shown that if the wavelet function is complex and its real and imaginary parts are Hilbert pairs, then the wavelet transform is shift-invariant and it is directional in higher dimensions. This concept was exploited to design steerable filter banks in [2]. Dual-tree complex wavelet is a new transform, which uses this concept to design oriented and shift-invariant filter banks [3]. In the Dual-tree complex wavelet, the amount of redundancy introduced into the original signal is $2^d - 1$, where d is the dimension of the signal.

There are some papers in the literature regarding the design of Hilbert transform pairs, without introducing any redundancy into the wavelet coefficients [4] [5]. The problem with these methods is that, they introduce serious bumps, which are distributed on the wrong side of the power spectrum. In contrast, due to the specific power spectrum of the filters in the proposed filter bank, the bumps are concentrated at high frequencies, which can easily be rejected by a lowpass filter.

1.1. 3-Band Filter Bank

In the 3-Band orthogonal wavelet transform, we have one scaling function φ and two wavelet functions ψ_1 and ψ_2 , which are related through the following equations:

$$\begin{aligned}\varphi(t) &= \sqrt{3} \sum_k h_0(k) \varphi(3t + k), \\ \psi_1(t) &= \sqrt{3} \sum_k h_1(k) \varphi(3t + k), \\ \psi_2(t) &= \sqrt{3} \sum_k h_2(k) \varphi(3t + k),\end{aligned}$$

where $h_i(n)$, $i \in \{1, 2, 3\}$, are three different filters that constitute the 3-band synthesis and analysis filter-banks as shown in Figure 1. In the case of the orthogonal wavelet, the synthesis filters are given by $\tilde{h}_i(k) = h_i^*(N - k - 1)$, $i \in \{1, 2, 3\}$, where h^* is the complex conjugate of h and N is the length of the filter.

In order to have a complete orthogonal transform, the scaling and the wavelet functions must satisfy the shift orthogonal condition. We can express this condition as the

following equation:

$$\sum_k h_i(k)h_j(3n+k) = \delta(n)\delta(i-j), \quad i, j \in \{1, 2, 3\}. \quad (1.1)$$

An interesting property applicable to wavelet functions, which is very useful in signal processing applications, is the moment cancellation property. If the wavelet functions cancel k moments,

$$\int t^l \psi_i(t) dt = 0, \quad i \in \{1, 2\}, \quad 0 \leq l < k,$$

then equivalently they have k zeros at $z = 1$ of the Z plane. Then we have

$$H_i(z) = \left(\frac{1 - z^{-1}}{2} \right)^k G_i(z), \quad i \in \{1, 2\}. \quad (1.2)$$

The moment cancellation property implies the following form on h_0 :

$$H_0(z) = \left(\frac{1 + z^{-1} + z^{-2}}{3} \right)^k G_0(z). \quad (1.3)$$

1.2. Linear Phase Filters

One of the most important properties of the filters which can be applied to 3-band filter banks is linearity of the phase. The phase of the signals which are filtered using the linear phase filters is not perturbed, which means all frequency components of the signal are shifted equally. The filter $h(t)$, which has the linear phase property, satisfies the following equation:

$$h(n) = \exp(i\theta)h^*(N-1-n), \quad 0 \leq n < N-1,$$

where N is the length of the filter and θ is an arbitrary variable between zero and 2π .

The following two special kinds of the linear phase filters are used in this paper:

1. Real filter with $\theta = 0$ and N to be odd,
2. Complex filter with $\theta = \frac{\pi}{2}$.

In the first case, N is implied to be odd, otherwise the filter has one or more zeros at $z = -1$, which is undesirable for our filter bank design procedure. In the second case, if we consider the filters $h_r(n)$ and $h_i(n)$ as the real and imaginary parts of the filter $h(n)$, respectively, then $h_r(n) = -h_i(N-1-n)$, $0 \leq n < N-1$.

2. Proposed 3-band Filter Bank

2.1. Filter Bank Characteristics

The ideal normalized power spectrum of the filters in the filter bank that satisfies all desirable characteristics, such as having the Hilbert-pairs wavelet filters and introducing no bumps on the wrong side of the power spectrum, is shown in Figure 2. This filter bank introduces no redundancy because one of the wavelet filters is the complex conjugate of the other, so the resulting coefficients of one filter is the complex conjugate of the other filter, and we can discard them in further analysis.

In a specific level and type of the filter bank, if we move down-sample and up-sample operations to the output of the analysis filter bank and to the input of the synthesis filter bank, respectively, then the cascaded filter transform function is retained. Figure 3 shows the simplified schematic of this operation in a specific level and type. For example, if we consider level 2 and filter type $H_1(z)$, then $M = 3^2$, $A(z) = H_0(z)H_1(z^3)$ and $B(z) = \tilde{H}_0(z)\tilde{H}_1(z^3)$.

The normalized power spectrum of different filter types from level 1 to level 3 for a designed filter bank are shown in Figure 4(a)-4(c). As we can see from this figure, due to the special frequency response of the filter h_0 that has a peak at $\omega = \pi$, the resulting filters at different levels are one-sided and they do not produce serious bumps on the wrong side of the frequency axis. As we can see, the bumps are in the same frequency direction and are concentrated at high frequency components around $\omega = \pi$.

These bumps can be easily rejected by placing symmetric lowpass filters before the analysis and after synthesis filter banks to annihilate high frequency components. The resulting power spectrum of the filters, after placing this lowpass filter, are shown in Figure 4(d)-4(f). The passband of the lowpass filter is around 0.5π so by placing this lowpass filter, we deviate the perfect reconstruction property of the filter bank. If the lowpass filter is considered as a part of continuous-to-discrete and discrete-to-continuous converters, then the sampling frequency must be computed such that, considering the input signal has finite bandwidth, the sampled signal contains ALL the information of the signal without any distortion.

In the ideal case, without considering this lowpass filter, the sampling frequency can be computed using Nyquist's theorem, i.e. the sampling rate must exceed twice the highest frequency of the signal, which is called the Nyquist frequency. In the non-ideal case, an anti-aliasing filter must be applied before the sampling part. In this case, the sampling frequency can be calculated using the following equation:

$$f_s \geq f_n + 2B_{tr},$$

where f_n is the Nyquist frequency and B_{tr} is the transient band of the anti-aliasing filter.

When using a discrete time lowpass filter after a continuous-to-discrete converter, we can compute another constraint for avoiding distortion. The sampling rate must be computed in such a way that the normalized bandwidth of the analog signal be equal to

the passband of the lowpass filter. Therefore, the following constraint is computed:

$$f_s \geq \frac{f_n}{2B_{low}},$$

where B_{low} is the normalized passband of the lowpass filter (which is around 0.5). In this case, the amount of sampling frequency increase with respect to the common sampling is

$$R = \frac{\frac{f_n}{2B_{low}}}{f_n + 2B_{tr}}.$$

For comparison, let the transient band of the anti-aliasing filter be half of the signal bandwidth and the normalized passband of the lowpass filter be 0.5, then $R = 1.33$. We can see that the amount of sampling rate increase is not very much. In addition, natural signals decay very fast with frequency increase; therefore if we deviate a little from this sampling rate constraint, the amount of distortion introduces into signal is not very much. We will see this in the second part of the simulation results.

In the extension to higher dimensions, the tensor product is applied to the wavelet and scaling functions. In 2-D, say, this product produces one real scaling function and eight traditional, separable wavelet functions. Since the wavelet filters are one-sided, the resulting wavelet functions in higher dimensions are also one-sided and therefore they are directional. Half of the wavelet functions are complex conjugate of the other half and therefore in higher dimensions, again, the filter bank introduces no redundancy.

As explained in [6], we choose to retain the coefficients of only one level and set all the others to zero. If the reconstructed signal from these coefficients is free of aliasing then we define the transform to be shift invariant at that level. In order to have the shift-invariance property in our filter bank, it is sufficient that the cascaded analysis and synthesis filters at level j have frequency band less than $\frac{2\pi}{3^j}$ and as we can see in Figure 4(d)-4(f), the proposed filter bank approximately satisfies this requirement.

Now, suppose we retain the coefficients of single level and single type. In this case, we use the equation introduced in [6] to quantify the shift dependence of a transform, which is defined as the ratio of the energy of an unwanted aliasing transfer function to the energy of the wanted transfer function, and is given by:

$$R_a = \frac{\sum_{k=1}^{M-1} \mathcal{E} \{A(W^k z) B(z)\}}{\mathcal{E} \{A(z) B(z)\}}, \quad (2.1)$$

where $\mathcal{E} \{U(z)\}$ calculates the energy, $\sum_r |u_r|^2$, of the impulse response of a z-transfer function, $U(z) = \sum_r u_r z^{-r}$ and $W = e^{i2\pi/M}$.

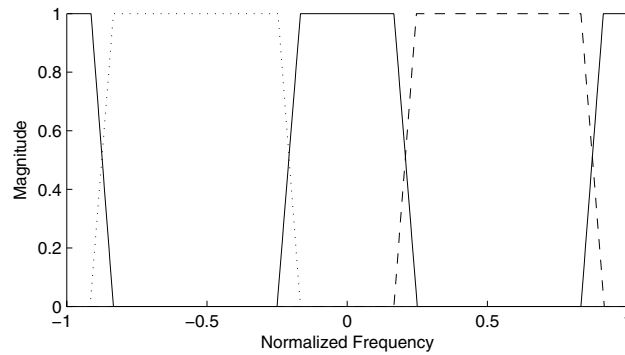


Figure 2: Proposed ideal normalized power spectrum of the filters in the 3-band filter bank.

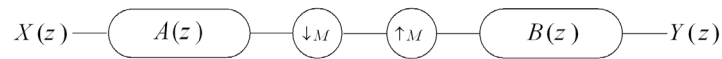


Figure 3: Simplified configuration if the coefficients from just one level and one type are retained.

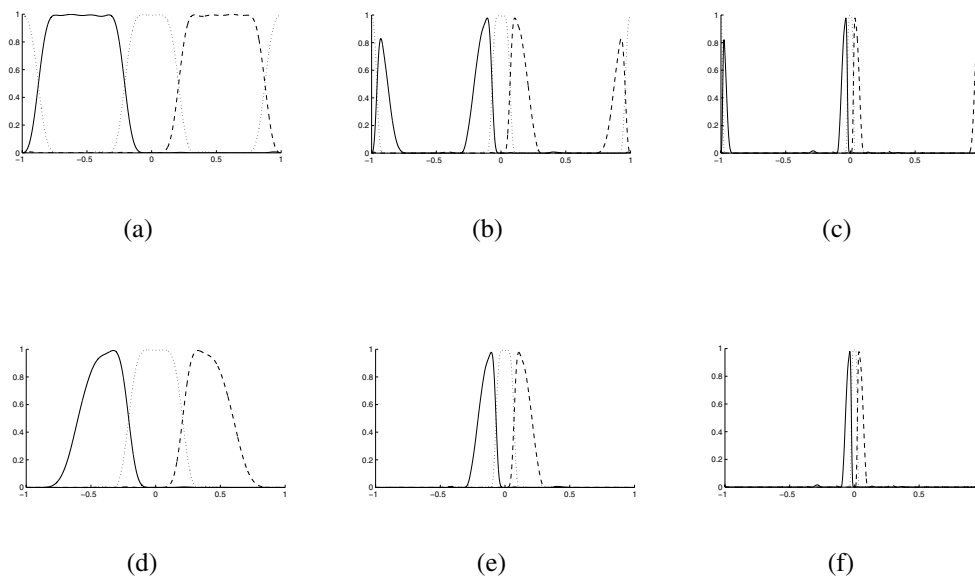


Figure 4: Level 1 to 3 of the filters power spectrum in the proposed filter bank (a-c) without (d-f) by applying the lowpass filter that removes frequencies higher than 0.8π . The filters are linear phase, have length 21 and cancel 3 moments.

2.2. Filter Bank Design Procedure

There exist different methods in the literature for designing orthogonal M-band filter banks [7]. In lots of these methods, there are some difficulties in imposing the regularity condition or the vanishing moment property in the design procedure. Kok [8] proposed a time domain design technique for designing linear phase orthogonal filter banks with high regularity and good stopband characteristics. In this part we explain about the modification of this algorithm in order to use it for designing of our filter bank.

We want to design an orthogonal filter bank which consists of one real filter $h_0(n)$ and two complex conjugate filters $h_c(n)$ and $h_c^*(n)$. If we consider

$$h_c(n) = \sqrt{\frac{1}{2}} \times (h_1(n) + ih_2(n)), \quad (2.2)$$

then for having a complete orthogonal transform, $h_0(n)$, $h_1(n)$ and $h_2(n)$ must satisfy the shift orthogonal condition expressed in Equation 1.1. Define the impulse response vectors \mathbf{h}_i of the filters in the filter bank by the following equation:

$$\mathbf{h}_i = \begin{pmatrix} h_i(0) \\ \vdots \\ h_i(N-1) \end{pmatrix}, \quad i \in \{1, 2, 3\},$$

where N is the length of the filters.

Define $\mathbf{Q}_l \in \mathbb{R}_{N \times N}$ as

$$[\mathbf{Q}_l]_{i,j} = \begin{cases} 1, & i - j = 3l, \\ 0, & \text{otherwise.} \end{cases}$$

Thus the shift orthogonal condition expressed in Equation 1.1 can be rewritten as

$$\mathbf{h}_i^T \mathbf{Q}_l \mathbf{h}_j = \delta(i - j) \delta(l).$$

The moment cancellation property expressed in Equation 1.2, can be easily expressed in terms of the impulse response vectors. If we want to have up to K vanishing moments and the filters have length N , then the filter g_0 in Equation 1.2 has length $N_{g_0} = N - 2K$. Define a matrix sequence $\mathbf{U}_k \in \mathbb{R}_{N_{g_0} + 2k \times N_{g_0} + 2(k-1)}$ as

$$[\mathbf{U}_k]_{i,j} = \begin{cases} \frac{1}{3}, & 0 \leq i - j < 3, \\ 0, & \text{otherwise.} \end{cases}$$

Thus, $\mathbf{h}_0 = \mathbf{U}_K \mathbf{U}_{K-1} \dots \mathbf{U}_1 \mathbf{g}_0$, where $\mathbf{g}_0 \in \mathbb{R}_{N_{g_0} \times 1}$ is the impulse response vector of the filter $G_0(z)$. Since $g_0(n)$ is a linear phase filter, it must satisfy the even-symmetric property described in part B of the introduction. This even-symmetric property can

be expressed easily as a matrix equation $\mathbf{g}_0 = \mathbf{S}\mathbf{g}_0^*$, where $\mathbf{g}_0^* \in \mathbb{R}_{N_{g_0}^* \times 1}$ and $N_{g_0}^* = (N_{g_0} - 1)/2$. The matrix $\mathbf{S} \in \mathbb{R}_{N_{g_0} \times N_{g_0}^*}$ is defined as

$$[\mathbf{S}]_{i,j} = \begin{cases} 1, & j = i \text{ and } i \leq N_{g_0}^* & \text{or} \\ & j = N_{g_0} - i + 1 \text{ and } i > N_{g_0}^* + 1 & \text{or} \\ & i = N_{g_0}^* + 1, & \\ 0, & \text{otherwise.} \end{cases}$$

The moment cancellation property can be applied to the filter $h_c(n)$. If the filter $h_c(n)$ cancels K moments, it has K zeros at $z = 1$ and therefore its real and imaginary parts have K zeros at $z = 1$, consequently Equation 1.3 holds true for $h_1(n)$ and $h_2(n)$ in Equation 2.2. If the filters have length N , for imposing K moment cancellation property, the filters $g_i(n)$, $n \in \{1, 2\}$ in the equation will have length $N_{g_1} = N - K$. Define a matrix sequence $\mathbf{V}_k \in \mathbb{R}_{N_{g_1} + k \times N_{g_1} + (k-1)}$ as

$$[\mathbf{V}_k]_{i,j} = \begin{cases} \frac{1}{2}, & j = i, \\ \frac{-1}{2}, & j = i - 1, \\ 0, & \text{otherwise.} \end{cases}$$

Thus $\mathbf{h}_i = \mathbf{V}_K \mathbf{V}_{K-1} \cdots \mathbf{V}_1 \mathbf{g}_i$, $i \in \{1, 2\}$, where $\mathbf{g}_i \in \mathbb{R}_{N_{g_1} \times 1}$ is the impulse response vector of the filter $G_i(z)$. Since the filter $h_c(n)$ is linear phase, so $h_1(n) = -h_2(N-1-n)$. And therefore $g_1(n)$ and $g_2(n)$ are related through the following relation:

$$g_2(n) = \begin{cases} g_1(N_{g_1} - n - 1), & K \text{ is odd,} \\ -g_1(N_{g_1} - n - 1), & K \text{ is even.} \end{cases}$$

The complex filter stopband power in a given frequency, $|H_c(e^{j\omega})|^2$, can be expressed in terms of the impulse response vector as

$$|H_c(e^{j\omega})|^2 = \mathbf{h}_c^T \mathbf{E}(\omega) \mathbf{E}^T(\omega) \mathbf{h}_c$$

where $\mathbf{E}^T(\omega) = [e^{i\omega} \ e^{2i\omega} \ \dots \ e^{Ni\omega}]$. Consider $\mathbf{M}(\omega) = \mathbf{E}(\omega) \mathbf{E}^T(\omega) = \mathbf{M}_{re}(\omega) + i\mathbf{M}_{im}(\omega)$, where $\mathbf{M}_{re}(\omega)$ and $\mathbf{M}_{im}(\omega)$ are symmetric and antisymmetric matrices, respectively. If h_c is expressed in terms of h_1 and h_2 as in Equation 2.2, then the complex filter stopband power in that frequency, can be expressed as

$$|H_c(e^{j\omega})|^2 = \mathbf{h}_1^T \mathbf{M}_{re}(\omega) \mathbf{h}_1 + \mathbf{h}_2^T \mathbf{M}_{re}(\omega) \mathbf{h}_2 + 2\mathbf{h}_2^T \mathbf{M}_{im}(\omega) \mathbf{h}_1.$$

The same procedure can be used for the computation of the stopband power of the filter h_0 in a given frequency, that leads to the following equation:

$$|H_0(e^{j\omega})|^2 = \mathbf{h}_0^T \mathbf{M}_0(\omega) \mathbf{h}_0. \quad (2.3)$$

The design cost function is given by

$$\Phi = \sum_{m=0}^2 \sum_l \sum_{i=0}^2 \{ \mathbf{h}_i^T \mathbf{Q}_l \mathbf{h}_m - \delta(l)\delta(m-i) \}^2 + \alpha \{ \mathbf{h}_0^T \mathbf{M}_0(\omega_1) \mathbf{h}_0 + \mathbf{h}_1^T \mathbf{M}_{re}(\omega_2) \mathbf{h}_1 + \mathbf{h}_2^T \mathbf{M}_{re}(\omega_2) \mathbf{h}_2 + 2\mathbf{h}_2^T \mathbf{M}_{im}(\omega_2) \mathbf{h}_1 \}, \quad (2.4)$$

where α is the weighting coefficient and the stopband power is calculated at those frequencies ω_1 and ω_2 that maximize it. For this purpose, the stopband is sampled uniformly and the stopband power is evaluated at these sampled frequencies. We use a gradient descend algorithm for minimizing the cost function. At every iteration, the weighting coefficient α should decrease such that the optimized filters satisfy the shift orthogonal condition. This iteration will terminate when the cost of the shift orthogonal condition expressed in the first line of Equation 2.4 becomes sufficiently small ($\approx 10^{-6}$).

3. Simulation Results

3.1. Filter Design

We use the aforementioned procedure for designing two different filter banks: one with filters of length 15 and 2 vanishing moments and one with filters of length 21 and 3 vanishing moments. The normalized power spectrum of the filters in dB and their impulse responses are shown in Figure 5, and the filter coefficients are given in Table 1. As we can see, the designed linear phase orthogonal filter banks with high vanishing moment have good spectral separation and high stopband attenuation. But as mentioned before, the scaling filter has a peak at $\omega = \pi$ that can be solved easily by placing a lowpass filter before and after the filter bank. The frequency response of the designed filter bank with filters of length 21, before and after the application of the lowpass filter, were shown up to the third level in Figure 4. It is clear that in all levels, the filter bank produces nearly Hilbert transform pairs wavelet filters. In all the other simulation results, we assume that the lowpass filter is applied to the filter bank.

3.2. Examining the Amount of Distortion

As explained before, we apply the lowpass filter before the analysis and after the synthesis filter banks, therefore we deviate from the perfect reconstruction condition. To examine the amount of distortion introduced into the signal, we apply three levels of the filter bank with the lowpass filter to some images of the USC database [9], and the resulting PSNRs (peak signal to noise ratio) of the reconstructed signals are given in Table 2. As we can see, the PSNR are very high. Therefore, we can consider our filter bank as a nearly perfect reconstruction filter bank on natural signals.

3.3. Examining Directionality

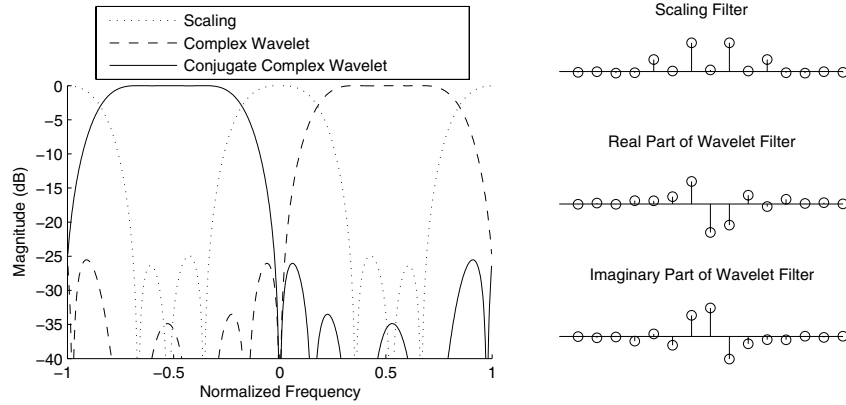
The complex filters in higher dimensions can provide good directional selectivity. For example, the impulse response of the 2-D filters at level 2 are shown in Figure 6. As we

Table 1: Designed filter coefficient.

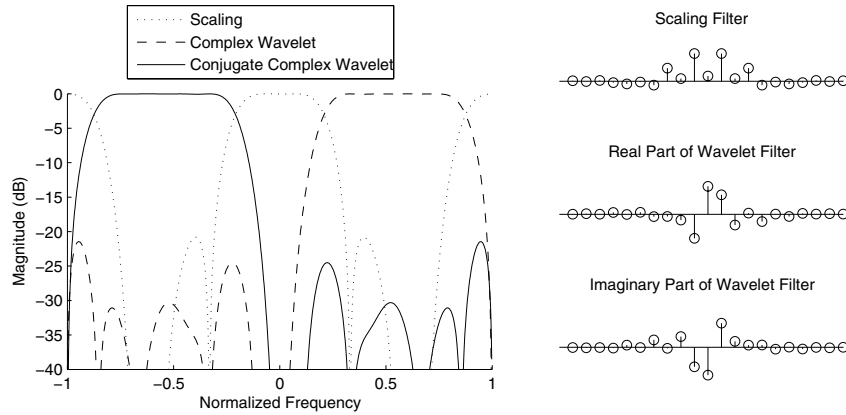
Filter length = 15		Filter length = 21	
Real filter h_0	Complex filter h_c	Real filter h_0	Complex filter h_c
		-0.0124	-0.0002 + 0.0041i
		0.0062	-0.0095 + 0.0090i
		-0.0184	-0.0014 + 0.0032i
-0.0195	-0.0046 - 0.0018i	0.0306	-0.0280 + 0.0134i
-0.0028	0.0160 - 0.0205i	0.0611	0.0024 - 0.0351i
-0.0373	-0.0050 - 0.0079i	0.0171	-0.0304 + 0.0042i
-0.0271	0.0530 - 0.0753i	0.0883	0.0372 - 0.1169i
0.2735	0.0504 + 0.0402i	-0.2966	0.0352 + 0.0177i
0.0127	0.1180 - 0.1403i	-0.0589	0.0938 - 0.1716i
0.6495	0.3612 + 0.3391i	-0.6231	0.3841 + 0.3107i
0.0369	-0.4554 + 0.4554i	-0.1181	-0.4446 + 0.4446i
0.6495	-0.3391 - 0.3612i	-0.6231	-0.3107 - 0.3841i
0.0127	0.1403 - 0.1180i	-0.0589	0.1716 - 0.0938i
0.2735	-0.0402 - 0.0504i	-0.2966	-0.0177 - 0.0352i
-0.0271	0.0753 - 0.0530i	0.0883	0.1169 - 0.0372i
-0.0373	0.0079 + 0.0050i	0.0171	-0.0042 + 0.0304i
-0.0028	0.0205 - 0.0160i	0.0611	0.0351 - 0.0024i
-0.0195	0.0018 + 0.0046i	0.0306	-0.0134 + 0.0280i
		-0.0184	-0.0032 + 0.0014i
		0.0062	-0.0090 + 0.0095i
		-0.0124	-0.0041 + 0.0002i

Table 2: PSNR of reconstructed signal.

Image	PSNR
Boat	57.58
Lenna	58.30
Baboon	60.18
Beach	55.80
Tree	55.77
Pepper	57.75
Cameraman	57.75



(a)



(b)

Figure 5: Frequency and impulse responses of the filters in the filter bank (a) filter length =15 and (b) filter length = 21.

can see in this figure, these filters are highly oriented in 0° , $\pm 45^\circ$ and 90° and the real and complex parts of the complex filter constitute Gabor-like filters. In another experiment, we apply the proposed filter bank on a disk image and the resulting absolute value of the wavelet coefficients at two different levels and different types are shown in Figure 7. As we can see, the filters even at the first level are oriented.

3.4. Examining Shift-Invariance

It is interesting to test the shift-invariance performance based on Equation 2.2. For the designed filter bank with the filters of length 15 and length 21, \mathbf{R}_a is calculated and is

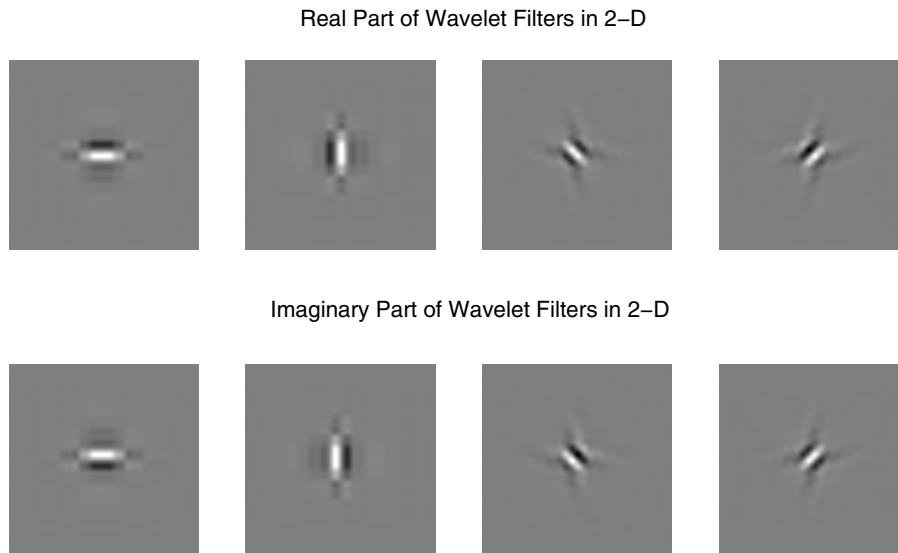


Figure 6: Impulse response of 2-D filter bank at level 2. Filter bank produces 4 oriented filters.

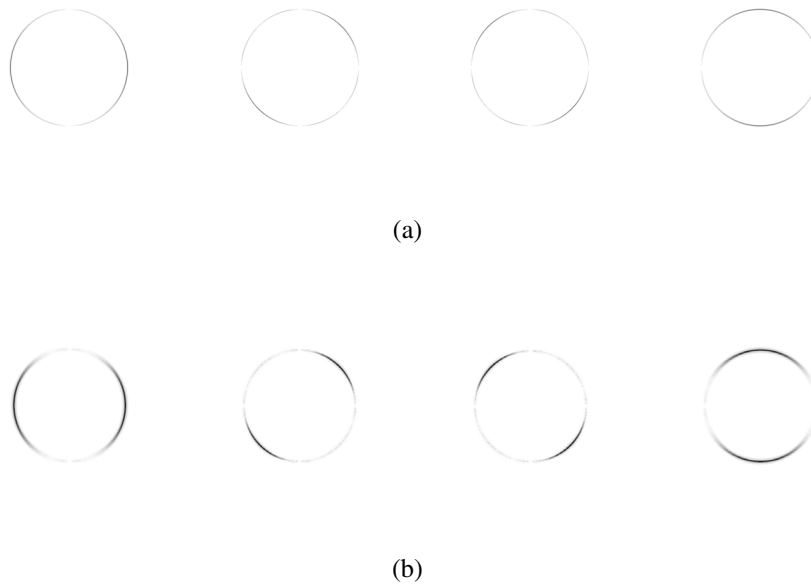


Figure 7: Absolute value of filtered disk image coefficients of different types (a) in first level (b) in second level.

Table 3: Calculated Shift Dependence criterion for Different Filters.

Filters:	Proposed filter bank		Dual-Tree Complex Wavelet	Traditional, separable DWT
	Length 15	Length 21		
Wavelet filter				
Level 1	-57.18	-58.93	$-\infty$	-9.40
Level 2	-34.76	-42.26	-31.40	-3.54
Level 3	-24.53	-32.49	-27.93	-3.53
Level 4	-23.42	-31.94	-31.13	-3.52
Scaling filter				
Level 1	-48.26	-60.64	$-\infty$	-9.40
Level 2	-33.23	-41.48	-32.50	-9.38
Level 3	-32.43	-40.73	-35.88	-9.37
Level 4	-31.57	-40.63	-37.14	-9.37

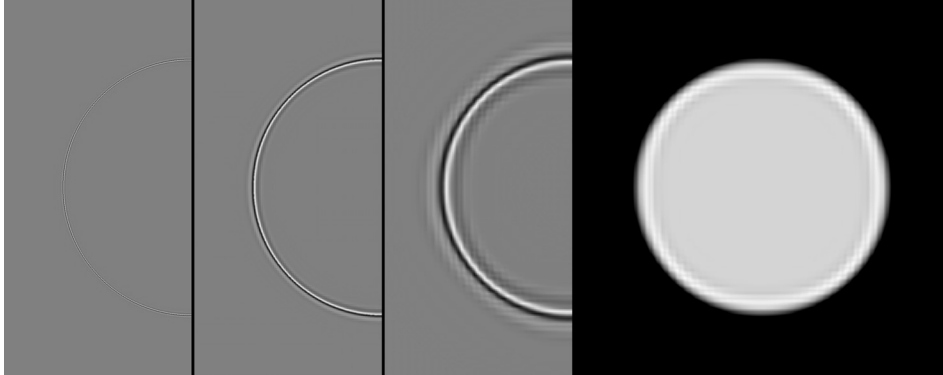


Figure 8: From left to right: reconstructed images of wavelet filters from level 1 to 3 and reconstructed image of scaling filter of level 3 (for saving space, only half of images are shown.)

shown in Table 3. For the sake of comparison, we present the best result among different designs of Dual-tree complex wavelet filters in [6] and also the result of traditional, separable DWT (scaling and wavelet filters of lengths are 19 and 13). Here \mathbf{R}_a is represented in dB , using $10 \log \mathbf{R}_a$. It is clear that the proposed filter bank has an excellent shift-invariance property which is comparable to the Dual-tree complex wavelet transform proposed by Kingsbury [6]. As an illustrative example, we construct the image of only one level and the reconstructed images are shown in Figure 8. One can see that transformed images are shift-invariant and free of aliasing.

4. Conclusion

In this paper, we proposed a new filter bank with Hilbert-pairs wavelet filters. We also proposed a time domain technique for designing the linear phase orthogonal filter banks that leads to filters with good stopband characteristics and a high vanishing moment property. As it was seen in the simulations, the proposed filter bank is shift-invariant and oriented in higher dimensions. In addition, the filter bank does not introduce any redundancy and is separable in higher dimensions.

Acknowledgements

Professor Vaillancourt is to be thanked for his careful reading of this work. An anonymous reviewer is gratefully acknowledged for his/her fruitful comments on the work.

References

- [1] Selesnick, I. W., Baranuick, R. G., and N. G. Kingsbury, 2005, The dual-tree complex wavelet transform, *IEEE Sig. Proc. Mag.*, 22(6), pp. 123–151.
- [2] Somincelli, E. P., Freeman, W. T., Adelson, E. H., and D. J. Heeger, 1992, Shiftable multi-scale transforms, *IEEE Trans. Inform. Theory*, 38(2), pp. 587–607.
- [3] Selesnick, I. W., 2001, Hilbert transform pairs of wavelet bases, *IEEE Signal Processing Letters*, 8(6), pp. 170–173.
- [4] van Spaendonck, R., Baraniuk, T. B. R., and M. Vetterli, 2003, Orthogonal hilbert transform filter banks and wavelets, in *Proc. IEEE Int. Conf. Acoust., Speech, Signal Processing*, 6, pp. 505–508.
- [5] Fernandes, F., Wakin, M., and R. Baraniuk, 2004, Non-redundant, linear-phase, semi-orthogonal, directional complex wavelets, in *Proc. IEEE Int. Conf. Acoust., Speech, Signal Processing*, 2, pp. 953–956.
- [6] Kingsbury, N. G., 2001, Complex wavelet for shift invariant analysis and filtering of signals, *J. of Appl. Comp. Harmonic Analysis*, 10(3), pp. 234–253.
- [7] Strang, G. and T. Nguyen, 1997, *Wavelet and Filter Banks*, 2nd ed. Wellesly, MA: Wellesley-Cambridge Press.
- [8] Kok, C. W., Ikehara, M., and T. Q. Nguyen, 2000, Design and factorization of fir paraunitary filter banks given several analysis filters, *IEEE Trans. Signal Processing*, 48(7), pp. 2157–2161.
- [9] Usc-sipi image database, university of Southern California. Available: <http://sipi.usc.edu/database/Database.html>.